

Classifying sleep states using persistent homology and Markov chain: a Pilot Study

Sarah Tymochko, Kritika Singhal, and Giseon Heo

Abstract Obstructive sleep Apnea (OSA) is a form of sleep disordered breathing characterized by frequent episodes of upper airway collapse during sleep. Pediatric OSA occurs in 1-5% of children and can related to other serious health conditions such as high blood pressure, behavioral issues, or altered growth. OSA is often diagnosed by studying the patient’s sleep cycle, the pattern with which they progress through various sleep states such as wakefulness, rapid eye-movement, and non-rapid eye-movement. The sleep state data is obtained using an overnight polysomnography test that the patient undergoes at a hospital or sleep clinic, where a technician manually labels each 30 second time interval, also called an “epoch,” with the current sleep state. This process is laborious and prone to human error. We seek an automatic method of classifying the sleep state, as well as a method to analyze the sleep cycles. This article is a pilot study in sleep state classification using two approaches: first, we’ll use methods from the field of topological data analysis to classify the sleep state and second, we’ll model sleep states as a Markov chain and visually analyze the sleep patterns. In the future, we will continue to build on this work to improve our methods.

Sarah Tymochko

Dept. of Computational Mathematics, Science and Engineering, Michigan State University, East Lansing, MI, e-mail: tymochko@egr.msu.edu

Kritika Singhal

Dept. of Mathematics, The Ohio State University, Columbus, OH, e-mail: k2singhal@gmail.com

Giseon Heo (corresponding author)

School of Dentistry; Department of Mathematical and Statistical Sciences, University of Alberta, Edmonton AB T6G 1C9, Canada. e-mail: gheo@ulberta.ca

1 Introduction

Obstructive sleep apnea (OSA) is a chronic condition characterized by frequent episodes of upper airway collapse during sleep. Pediatric OSA is a serious health problem; even mild forms of untreated pediatric OSA may cause high blood pressure, changes to the heart, behavioral challenges, or alter the patients growth. The prevalence of childhood OSA is in the range of 1-5%. The gold standard for diagnosis of pediatric OSA is by overnight polysomnography (PSG) in a hospital or sleep clinic. PSG provides multi-channel time series, such as EEG, ECG, EOG, EMG, airflow, and SpO₂. In order to determine the sleep state, a sleep technician must manually assign the sleep state for each epoch (a 30 second interval) based on the PSG multi-channel time series. This is a laborious process which is subject to human error.

Following this labeling process, a sleep specialist determines the severity of OSA by assigning a *apnea hypopnea index (ahi)* based on the PSG time series and sleep patterns of a patient. The severity of OSA in children is categorised as *none* ($ahi < 1$), *mild* ($1 \leq ahi \leq 5$), *moderate* ($5 < ahi \leq 10$), or *severe* ($ahi > 10$).

There are three main types of sleep, wakefulness, rapid eye-movement (REM), and non rapid eye-movement (NREM). The NREM is further divided into three states: NREM1, NREM2, NREM3. REM sleep, brain waves are similar to waking. NERM1 is transition between waking and sleep, NREM 1-2 are refereed as Stage 1-2 (light sleep) and NERM3 is Stage 3 (deep sleep). For the majority of people, sleep begins with a short period of NREM1 then go to deeper sleep, and returning to REM. The progression through the various sleep stages is called a sleep cycle. The sleep cycle depends on age: 45-50 min for < 2 years, 50-60 min for 2-4 years, 60-80 min for 5-11 years, 80-100 min for 12-13 years and 90-120 min for > 13 years. The proportions of REM and NREM also depend on age, proportion NREM increases as get older. Roughly, 50-50% for newborn, 25-75% for 6-30 years old, and 20-80% for older than 30 years.

Seventy eight children at risk of OSA were recruited and had taken polysomnography (PSG). This project was approved by the Health Research Ethics Board of the University of Alberta (Pro00057638). As the objective of this article is exploring applications of persistent homology to multiple time series and understanding sleep stages and OSA severity, we will analyse a small subset of patients; eight patients and their PSG data. We selected two patients from each four OSA severity category. We present descriptive statistics of eight patients in the Table 1. The sleep state recorded at each 30 second interval (epoch) over the entire sleep duration of a patient can be represented in a *hypnogram*. The hypnograms of two patients, CF046 and CF050 are depicted in Figure 1.

As labeling sleep state based on PSG data is currently done manually, it would be useful to come up with automated sleep scoring mechanism. This would optimize the effort and time of the technician, as well as remove the human error from the labeling process. In this article, analyze time series variables from the PSG data using two separate approaches. The first approach, discussed in section 2, using a persistent homology based method to predict the sleep state for 30 second interval

	CF011	CF030	CF031	CF046	CF050	CF055	CF076	CF079
Wake	24.47	7.81	5.31	13.58	25.67	15.18	17.00	24.53
REM	14.16	19.22	17.93	11.22	10.48	17.24	13.70	8.41
NREM1	2.37	1.30	2.47	8.76	3.64	4.41	5.10	7.32
NREM2	40.27	41.58	35.50	32.43	32.73	41.92	41.60	40.26
NREM3	18.72	30.09	38.79	34.01	27.49	21.25	22.60	19.49
<i>ahi</i>	5.0	3.7	7.5	10.9	113.9	40.2	1.1	0.6
Age (yr)	9.2	4.1	4.1	9.7	13.7	13.7	9.8	17
Total sleep (hr)	9.13	10.88	9.11	9.51	7.80	8.51	8.33	8.43
Duration of sleep cycle (min)	60-70	50-60	50-60	60-70	90-120	90-120	60-70	90-120

Table 1: Percentage of each sleep stage, *ahi*, age at the time of PSG was taken, total # of sleep hours and duration of sleep cycle.

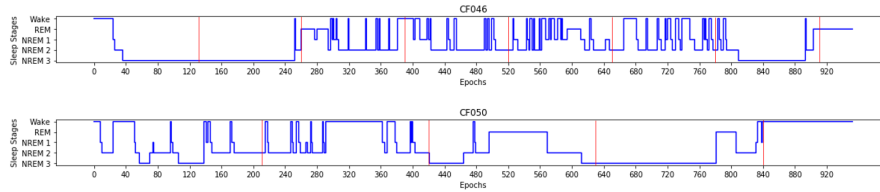


Fig. 1: Hypnograms of patients CF046 and CF050 with sleep cycles 65 min (130 epoch) and 105 min (210 epoch) respectively.

of three time series. For the second approach, in Section 3, we model sleep stage as 5-state Markov chain and visually inspect and sleep patterns of 8 patients. The goal is to explore both the automatic prediction of sleep states, as well as observing relationships between OSA and sleep patterns. We conclude our study with plan for future research.

2 Sleep State Analysis using Persistent Homology

The utilization of tools from topological data analysis (TDA) for time series analysis has recently become a popular line of research. The combination of these fields has resulted in new methods for quantifying periodicity and distinguishing behavior in time series data. PSG time series variables display different patterns for different sleep states. One proposed method of detecting these differences is using persistent homology, a well studied tool for quantifying the underlying structure of data. Persistent homology has been used to study time series data from many applications. Existing applications include studying machining dynamics [11, 12, 13], gene expression [21, 2], financial data [15], and video data [28, 26]. Additionally, [5] used

topological methods for time series analysis of sleep-wake states. Our goal is to explore the use of persistent homology to classify sleep states in PSG data. We also hope to see some variation in classification results that relate to the OSA severity of the patient.

As described in Sec. 1, we have 8 patients with varying severity of OSA. For each patient, we will consider three channels from the polysomnography data, specifically the central electrode on the sclape (C3), left eye movement (LEOG), and right eye movement (REOG). Each of these time series must be normalized by subtracting a reference electrode, M2 which placed on the mastoid. See Figure 2.

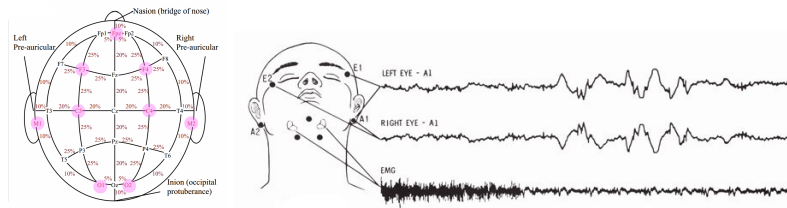


Fig. 2: (Left) The International 10/20 System of Electrode Placement. Image from sleeptechstudy.wordpress.com. (Right) EOG and EMG electrode placement. Image from [22]

2.1 Background

In this section, we'll present some necessary background information on persistent homology, time series analysis, and machine learning. Section 2.1.1 will cover the necessary background material, however for a more detailed overview, we refer the interested reader to [6, 9, 16, 18].

2.1.1 Persistent Homology

A standard tool from algebraic topology is homology, which studies topological features such as connected components, loops and voids. Given a space X , homology computes a group, $H_p(X)$, for each dimension $p = 0, 1, 2, \dots$. Each dimension contains information about the topological structure; specifically dimension 0 corresponds to connected components, dimension 1 corresponds to loops, and dimension 2 corresponds to voids. Here we'll focus on simplicial homology, but we must first define a few other concepts.

An n -simplex is defined as the convex hull of $n + 1$ affinely independent points. For example, a 0-simplex is a vertex, a 1-simplex is an edge, and a 2-simplex is a

triangle. The face of an n -simplex, σ , is defined as the convex hull of a nonempty subset of the vertices in σ . A simplicial complex \mathcal{K} is a space built from simplices that satisfies two properties: first, the intersection of any two simplices in \mathcal{K} must also be a simplex in \mathcal{K} and second, all faces of a simplex in \mathcal{K} must also be a simplex in \mathcal{K} .

For a simplicial complex \mathcal{K} , a p -chain, c , is a sum of p -simplices, σ_i in \mathcal{K} , with some coefficients a_i , $c = \sum a_i \sigma_i$. In this case, we're focusing on the simplified case of $a_i \in \mathbb{Z}_2$ as this is typically used for persistent homology. Here the collection of p -chains, or the chain group, denoted as $C_p(\mathcal{K})$, forms a vector space. The boundary map is a linear transformation between chain groups $\partial_p : C_p \rightarrow C_{p-1}$ that maps a p -simplex to the sum of its $(p-1)$ -dimensional faces. The sequence of boundary maps between chain groups

$$\cdots \xrightarrow{\partial_{p+1}} C_p \xrightarrow{\partial_p} C_{p-1} \xrightarrow{\partial_{p-1}} C_{p-2} \xrightarrow{\partial_{p-2}} \cdots$$

Within chain groups, we define a p -cycle $c \in C_p$ with empty boundary, $\partial_p(c) = 0$. Thus, the set of p -cycles is the kernel of the boundary map, $\ker(\partial_p)$. A p -boundary is a p -chain $c_p \in C_p$, that is the boundary of a $p+1$ -chain, $c_{p+1} \in C_{p+1}$, $c_p = \partial_{p+1}(c_{p+1})$. The set of p -cycles is the image of the boundary map $\text{im}(\partial_p)$. Then the p -th homology group is defined as

$$H_p(\mathcal{K}) = \ker(\partial_p) / \text{im}(\partial_{p+1}).$$

Persistent homology is a method of studying the homology of a space across different scales. In this case, we will use the Vietoris-Rips complex to create a simplicial complex out of the point cloud. The Vietoris-Rips complex is defined for a point cloud, X and a distance r , where for every finite set of k vertices with maximum pairwise distance at most r , the $(k-1)$ -simplex formed by those vertices is added to the complex. Then taking a range of distance values, $\{r_i\}$ we get a set of simplicial complexes $\{X_{r_i}\}$ where if $r_i \leq r_j$, then $X_{r_i} \subseteq X_{r_j}$. Thus, taking an increasing sequence of distance values, $0 \leq r_0 \leq r_1 \leq \cdots \leq r_n$ results in a nested sequence of simplicial complexes,

$$X_{r_0} \subseteq X_{r_1} \subseteq \cdots \subseteq X_{r_n} \quad (1)$$

called a filtration. The inclusions induce linear maps between the homology groups of each simplicial complex,

$$H_p(X_{r_0}) \rightarrow H_p(X_{r_1}) \rightarrow \cdots \rightarrow H_p(X_{r_n}). \quad (2)$$

These maps allow us to track how the homology changes through the filtration.

A p -dimensional feature is "born" at the distance value corresponding to the first time in the sequence of homology groups that we see that feature appear. More formally, γ is born at r_i if $\gamma \in H_p(X_{r_i})$ but $\gamma \notin H_p(X_{r_{i-1}})$. We say that a feature "dies" if it merges with an older feature. Specifically, a feature γ dies at r_j if it merges with a feature that has earlier birth time between $X_{r_{j-1}}$ and X_j . A persistence diagram is

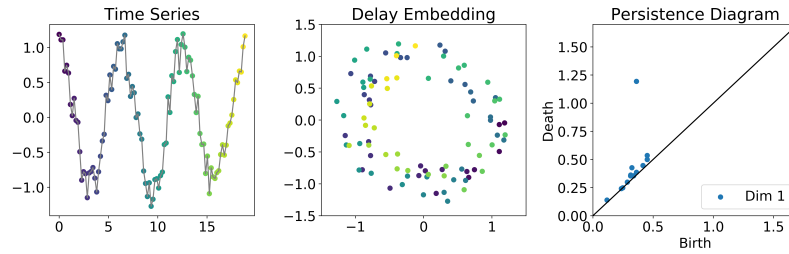


Fig. 3: Example time series (left), delay embedding with $d = 2$ and $\tau = 9$ (middle), and corresponding persistence diagram (right).

a method of recording this information, where a feature that is born at r_i and dies at r_j is represented by the point (r_i, r_j) .

Persistence diagrams provide concise and robust summaries of the topological features on various scales. However, these diagrams are not well suited for machine learning tasks. There are many methods, often called featurization methods, of converting the information in a persistence diagram into a vector. Once the diagram has been converted to a vector, it can be used in standard machine learning frameworks. In this paper, we'll use one featurization method called persistence images [1]. We will not go over the details of the method here, however an example can be seen in Fig. 4.

For implementation, we use scikit-tda python package [23] to compute persistent homology with ripser [27] and to transform the persistence diagrams into persistence images with the Persim library. For both of these computations, we use the default parameters.

2.1.2 Time Series Analysis

Now that we have established a framework for persistent homology, we need to convert time series data into a form that is amenable to this type of analysis. There are several existing methods to convert a time series into a point cloud. One popular method, called a delay embedding, leverages Takens' theorem [25]. Given a time series, $X(t)$, we select two parameters, a dimension $d \in \mathbb{Z}_{>0}$ and a delay, $\tau > 0$. The delay embedding is then defined as

$$\phi_{\tau,d} : X(t) \mapsto (X(t), X(t + \tau), X(t + 2\tau), \dots, X(t + (d - 1)\tau))$$

Takens' theorem proves that with the right parameters, this is in fact an embedding in the true mathematical sense as it preserves the underlying structure of the manifold. This embedding is sensitive to the choices of d and τ . To choose these parameters automatically, we use a method based on permutation entropy, as presented in [17]. Once the time series has been embedded as a point cloud with this

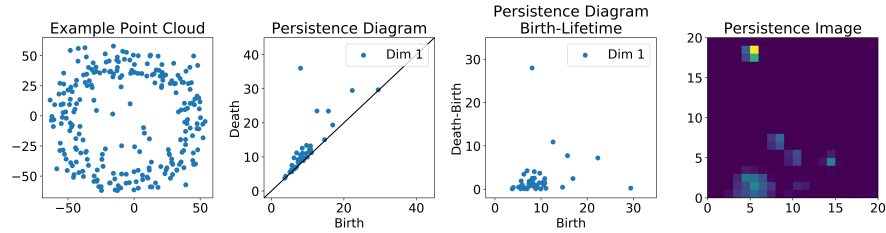


Fig. 4: Example of a point cloud with corresponding persistence diagram and persistence image. The persistence diagram must first be transformed into birth-lifetime coordinates, meaning a point (b, d) in the original diagram, is now plotted as $(b, d - b)$ in the birth-lifetime diagram. The persistence images method converts the birth-lifetime diagram into an image, represented as a 20×20 matrix. That matrix can be flattened into a 1×400 vector that can then be used for machine learning.

# of Classes	Labels
2	Wake, Sleep
3	Wake, REM, NREM (1, 2&3)
4	Wake, REM, Light Sleep (NREM 1&2), Deep Sleep (NREM 3)
5	Wake, REM, NREM 1, NREM 2, NREM 3

Table 2: Possible labels for 2, 3, 4 and 5 class classifications.

method, standard persistent homology can be applied. Figure 3 has an example of the delay embedding method along with the corresponding persistence diagram.

2.2 Results

To apply the methods described in Sec. 2.1, for each patient, we break the time series into non-overlapping 30 second intervals corresponding to the labeled epochs. Then for a given time series, we embed each 30 second interval separately using the Takens' embedding method and compute 1-dimensional persistence on the resulting point cloud. For each persistence diagram we create a feature vector using persistence images. Note we're only using 1-dimensional persistence diagrams because a time series with any periodic behavior will create a circular shape in the embedded point cloud. An example of this transformation from persistence diagram to feature vector can be seen in Fig. 4. We will test each of the three PSG channels for classification separately, in addition to testing all of them combined. We can test all of the channels together by computing their feature vectors with persistence images, and then concatenating the corresponding vectors for each epoch. Note that for our analysis, we keep the data separated by patient in order to compare based on *ahi* index as well.

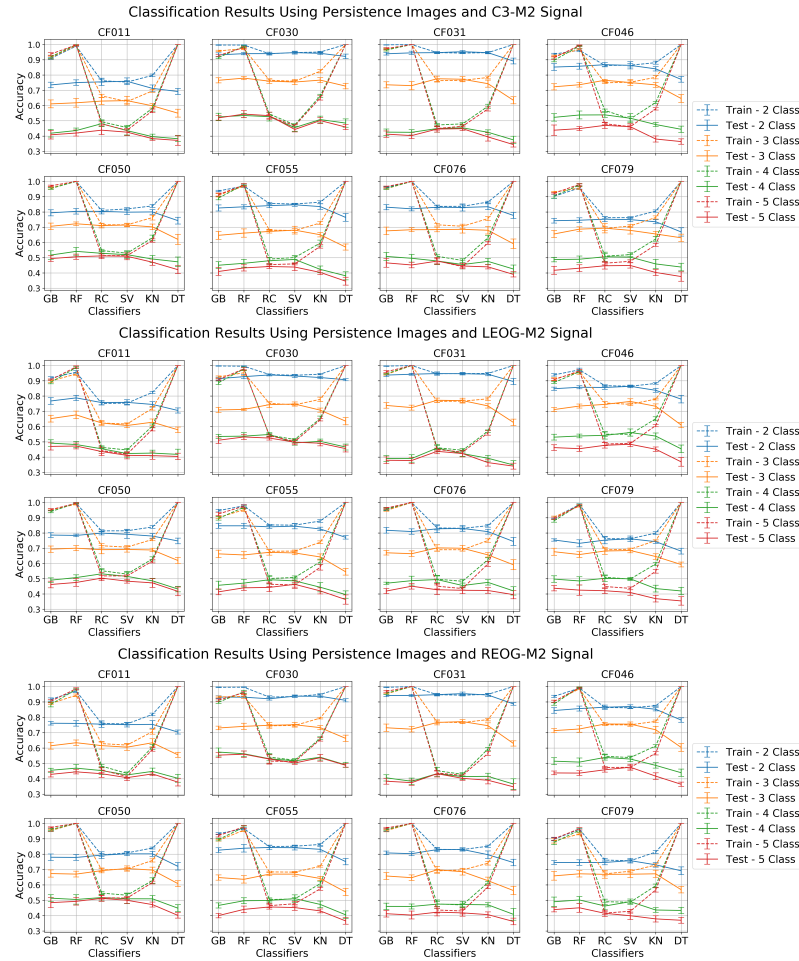


Fig. 5: Average classification accuracies using persistence images for 2, 3, 4 and 5 classes for each patient. Error bars are the standard deviation. Classifiers used are gradient boosting (GB), random forest (RF), ridge classification (RC), support vector classifier (SV), K-neighbors classifier (KN) and decision tree (DT).

For classification, we will test 2, 3, 4 and 5 class classification. The possible labels for each task are listed in Table 2. To perform the classification, we use the python package scikit-learn [19] to use six supervised machine learning algorithms: gradient boosting [7], random forest [3], ridge regression [10], support vector machines [24], k-nearest neighbors classifier [8], and decision tree [4]. For all of these classifiers, we use the default parameters. For each experiment, we reserve 33% for testing data and use the remaining for training. We also run each classification task 10 times and average the accuracies across all 10 runs. The average and standard

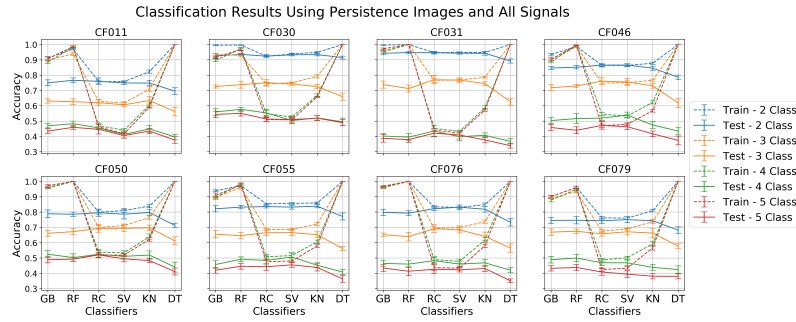


Fig. 6: Average classification accuracies using persistence images for 2, 3, 4 and 5 classes for each patient using all three signals. Error bars are the standard deviation. Classifiers used are gradient boosting (GB), random forest (RF), ridge classification (RC), support vector classifier (SV), K-neighbors classifier (KN) and decision tree (DT).

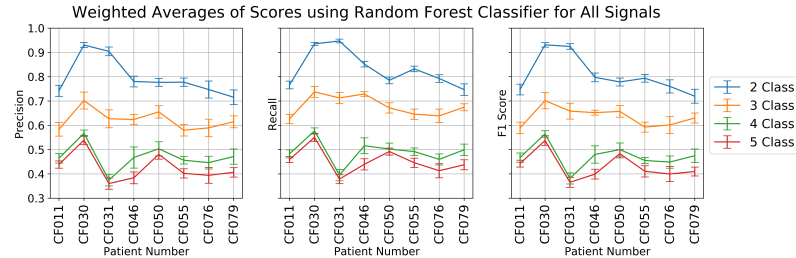


Fig. 7: Weighted average precision, recall and F1 scores for Random Forest classification for each patient using 2, 3, 4 and 5 classes. Error bars are the standard deviation.

deviation of the accuracies for all classification algorithms can be seen in Fig. 5 and Fig. 6.

From these results, we note that in Fig. 5, each of the signals provide similar results for each patient. Thus one signal does not seem to contain more information about the sleep state than the others. This is further emphasized by the fact that the results in Fig. 6 for all signals combined do not improve upon results from looking at a single signal. For all patients, all classifiers the training accuracies vary, with random forests performing above 90% for all patients, however the testing accuracies are about the same for a given number of classes. It is expected that the performance of the classifiers is worse for more classes. It appears that the 4 and 5 class classifications achieve relatively similar accuracies, while there is a big improvement reducing it to 3 classes.

Looking across patients, there are variations. In general, for patient CF030, the classification accuracies are generally higher than for other patients for all numbers

of classes. Patient CF079 seems to have the worst classification accuracies. However, these variations in classification accuracies do not seem to correlate with the *ahi* index.

Existing methods compared in [20] almost all achieve over 90% accuracies. However none of the methods mentioned use topological features. In direct comparison, the authors in [5] use similar persistent homology based approaches, however they use a different featurization method and they test their method across many databases. They perform three different classification tasks: (1) sleep vs. wake, (2) REM vs. NREM, and (3) wake vs. REM vs. NREM. For the first task, they report mean accuracies ranging from approximately 62-75% accuracy with across datasets. Their lowest reported accuracy, $62.6 \pm 17.0\%$, is from a dataset that contains patients with OSA. Our accuracies for the two class classification problem are over 70% for all patients. We acknowledge that we are only using 8 patients, while the datasets used in [5] are much larger, so it is not a direct comparison. However, the consistency of our results across these 8 patients with varying OSA severity seems promising that it would extend to larger datasets.

As shown in Table. 1, we have very imbalanced data, and thus reporting accuracy alone may not fully report the results. Thus, in Fig. 7 we report the weighted average for precision, recall and F1 score. Each of these scores is defined based on the number of true positives (TP), true negatives (TN), false positives (FP) and false negatives (FN):

$$\text{Precision} = \frac{TP}{TP + FP}, \quad \text{Recall} = \frac{TP}{TP + FN}, \quad \text{F1} = \frac{2 \cdot TP}{2 \cdot TP + FP + FN}$$

Each score is calculated for each class, then a weighted average is taken based on the number of samples with that class label. Note that if any class has no predicted samples, the score for that class is set to 0. These calculations are done with the scikit-learn implementations. We then take that weighted average for the 10 runs and take the average and standard deviation of those 10 values.

3 Visualizing Sleep Patterns of Eight OSA Patients

In this section, our objective is to understand and visualize sleep patterns of the eight patients in our data set. As we see in Figure 1, a hypnogram records the sleep state at each epoch over the entire sleep duration of a patient. In our data, since the patients sleep for different time durations, we have different number of total epochs for each patient. However, we want to compare the hypnograms epoch by epoch. Therefore, we normalize them by truncating at the minimum number of epochs of a patient. We can make some observations just by looking at the hypnograms, one being that the sleep pattern of patient CF046 looks very different from the others. Similarly, we observe that the initial sleep stages for patient CF050 are different from the rest of the patients, see Figure 13 in the appendix, where the hypnograms of the remaining patients are depicted. These observations therefore lead to the conjecture

that there is a relation between the sleep stage data and the severity of OSA in a patient. Therefore, we plan to use various statistical tools to study the sleep stage data and based on our results, determine the pairs of patients with same severity of OSA. This observation was made by one of authors, KS, who was blinded to the information of patients' OSA severity.

We consider three measures to inspect sleep patterns, namely transition probabilities, Cohen's κ , and Kullback-Leibler divergence. To do so, we model sleep as a discrete Markov chain with 5 states. Let $(X_t)_\mathbb{N}$ denote the stationary categorical process with state space $S = \{1, 2, 3, 4, 5\}$, corresponding to the sleep states **Wake(W)**, **REM(R)**, **NREM1(N1)**, **NREM2(N2)**, **NREM3(N3)**, and $\pi = (\pi_i, \dots, \pi_{i_5})$, denote the marginal distribution for each patient i . Table 3 shows the marginal distribution for the eight patients.

Patient	Marginal Distribution of (W, R, N1, N2, N3)	Order of frequencies
CF011	(0.247, 0.146, 0.023, 0.397 , 0.184)	$N2 > W > N3 > R > N1$
CF030	(0.078, 0.192, 0.013, 0.415 , 0.300)	$N2 > N3 > R > W > N1$
CF031	(0.052, 0.183, 0.030, 0.359, 0.375)	$N3 > N2 > R > W > N1$
CF046	(0.133, 0.110, 0.086, 0.319, 0.349)	$N3 > N2 > W > R > N1$
CF050	(0.270, 0.102, 0.035, 0.321 , 0.269)	$N2 > W > N3 > R > N1$
CF055	(0.148, 0.188, 0.043, 0.411 , 0.208)	$N2 > N3 > R > W > N1$
CF076	(0.170, 0.135, 0.050, 0.420 , 0.223)	$N2 > N3 > W > R > N1$
CF079	(0.243, 0.083, 0.072, 0.407 , 0.192)	$N2 > W > N3 > R > N1$

Table 3: Marginal Distributions π of all 8 patients

For time-homogeneous Markov chain $X_t, t \in \mathbb{N}$, the transition probability is defined as $P(X_t = j | X_{t-1} = i) := p_{ji}$ for any $i, j \in S$ and all $t \in \mathbb{N}$. We note that the sum of probabilities in each row equals to one, i.e. $\sum_{j \in S} p_{ji} = 1$. The transition probability matrix and a visual representation of the 5-state Markov chain of a patient is depicted in Figures 8 and 9.

	W	R	N1	N2	N3
W	0.85	0.004	0.104	0.04	0
R	0.082	0.882	0.035	0	0
N1	0.094	0.094	0.54	0.27	0
N2	0.048	0.004	0.012	0.925	0.009
N3	0.015	0	0	0.005	0.979

Fig. 8: Transition probability of CF079.

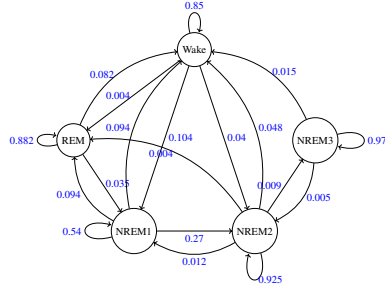


Fig. 9: Visual representation of Markov chain (CF079).

To analyse the serial dependence structure of sleep state, we calculate Cohen's κ at each lag k as recommended by [29]. Cohen's κ is analogous to auto-correlation function in real-valued process (continuous time series). It is defined as

$$\kappa(k) = \frac{\sum_{j \in \mathcal{S}} (P_{jj}(k) - \pi_j^2)}{1 - \sum_{j \in \mathcal{S}} \pi_j^2},$$

where $P_{ij}(k) = P(X_t = i, X_{t-k} = j)$. The range of Cohen's κ is $\left[-\sum_j \pi_j^2 / (1 - \sum_j \pi_j^2), 1\right]$. A positive (negative) value of $\kappa(k)$ means positive (negative) serial dependence, and a value of 0 means serial independence at lag k . The Cohen's $\kappa(k)$ plots for $k = 1, \dots, 130$, are depicted for two patients in Figure 10, and for all patients in Figures 12 and 14 of the appendix.

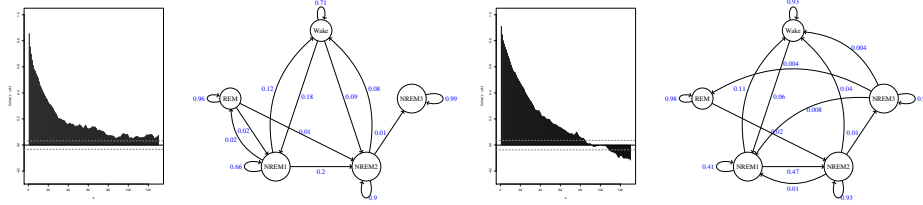


Fig. 10: (Left) Cohen's κ plots and representation of transition probabilities for patients CF046 (left) and CF050 (right).

We observe that Cohen's $\kappa(k)$ of patient CF050 is positive and gradually decreases until $k = 90$, and then decreases to -0.2 at lag $k = 130$, see Figure 10. This can be interpreted as each state tends to be followed by itself (but correlation decreases gradually), and then tends to flow from state to state. The Cohen's $\kappa(k)$ of CF046 is positive at every lag $k = 1, \dots, 130$, which means that the patient's sleep state is followed by itself. However, hypnogram of CF046 indicates that the patient stays at NREM 3 for long period of time during first, second and the last sleep cycles, while there is frequent flow between sleep states during the middle sleep cycle. Although, hypnogram and $\kappa(k)$ look different for CF046 and CF050, in terms of OSA severity, they are somewhat similar in that CF046 is moderate, and CF050 is severe.

We now compare transition probability matrices $\mathbb{P}^1, \dots, \mathbb{P}^8$ of the eight patients by calculating the Kullback-Leibler (KL) [14] divergence between probability distributions in each corresponding column in \mathbb{P} and \mathbb{P}' . As an example, KL between first row in each \mathbb{P} and \mathbb{P}' is $D_{kl}(\mathbb{P}_1 \parallel \mathbb{P}'_1) = \sum_i p_{i1} \ln(p_{i1}/p'_{i1})$. We now define Kullback-Leibler divergence between \mathbb{P} and \mathbb{P}' as

$$D_{kl}(\mathbb{P} \parallel \mathbb{P}') = \sum_i \sum_j p_{ji} \ln \frac{p_{ji}}{p'_{ji}}.$$

The KL divergence is asymmetric, the reason being that $\text{KL}(\mathbb{P} \parallel \mathbb{P}') \neq \text{KL}(\mathbb{P}' \parallel \mathbb{P})$. We present sum of the two, i.e. $\text{KL}(\mathbb{P} \parallel \mathbb{P}') + \text{KL}(\mathbb{P}' \parallel \mathbb{P})$, in Figure 11.

Ideally, KL divergence would be higher between no and severe patients. As we notice from the table in Figure 11, there is no clear pattern. The patient CF050 with

	CF079	CF076	CF030	CF011	CF031	CF046	CF055	CF050
CF079	0	1.41	1.59	1.84	0.91	1.02	1.08	2.00
CF076		0	1.50	0.82	1.14	0.77	0.61	0.82
CF030			0	2.96	1.28	1.27	0.56	1.35
CF011				0	0.89	2.19	1.23	1.56
CF031					0	1.34	0.85	1.94
CF046						0	0.57	1.52
CF055							0	0.78
CF050								0

Fig. 11: Kullback-Leibler divergence between 8 patients. OSA severity of CF079 & CF076: no, CF030 & CF011: mild, CF031 & CF046: moderate, CF055 & CF050: severe.

highest *ahi* has high divergence from the patient CF079 with the lowest *ahi* and it is similar to the patient, CF055 (high *ahi*) as well as CF076 (low *ahi*). In conclusion, transition probabilities, Cohen's κ , and KL-divergence were not able to distinguish patients with low *ahi* from those with high *ahi*.

In general, sleep patterns change through the night. At the beginning of sleep, a majority of people are in states mostly N2 and N3, with sporadic periods of N1 and short R periods. As the night progresses, the period of N3 becomes shorter, while N1 and N2 remain similar with longer R period. Both CF046 and CF050 don't follow the typical sleep patterns during sleep. The patient CF046 starts with a good sleep with a long period of N3 but after sleep cycle 2, frequent wake ups unable the patient to hit deep sleep until the morning. The pattern of CF050 is somewhat opposite to that of CF046; first frequent wake ups without falling in deep sleep during the early cycles, and then hit N3 during the last sleep cycle. Neither of these two patterns are considered as ideal sleep. As we might expect, the patterns of transition probabilities are different in sleep cycles of patients. See for example, the transition probabilities in each sleep cycle for two patients in Figures 15 and 16 in the appendix. We therefore observe that it would be more useful to incorporate sleep cycles while calculating Cohen's κ , transition probabilities, and KL divergences.

4 Conclusion and Future Research

In this paper, we first use a persistent homology approach for time series analysis to classify sleep states from three different PSG channels. Our classification accuracies range drastically based on the number of classes used. Additionally, the F1 scores reveal the underlying issue of class imbalance, which should be taken into account when considering our accuracies. In the future, we would like to further work on this class imbalance issue, possibly by subsampling the data to get relatively equal distribution of classes in order to determine if this method using persistent homology

is worth pursuing further. We'd also like to test to see if using other featurizations of persistence diagrams yield different results.

We modeled sleep stages as 5-state discrete first-order Markov chain and try to discern sleep patterns of eight OSA patients with different OSA severity using transition probabilities, Cohen's κ , and Kullback-Leibler divergence. These three measures were not able to discern patients with low *ahi* from those with high *ahi*. This was our naive attempt to understand any relationship between pattern of sleep stages and severity of OSA. Our next research goal is to analyse our data incorporating the sleep cycles. Furthermore, we plan to consider higher order Markov chain.

Acknowledgements This work was started at the second Women in Data Science and Mathematics workshop (WiSDM 2) in summer 2019, at The Institute for Computational and Experimental Research in Mathematics (ICERM), Brown University. We thank ICERM for the support. The authors would like to thank their fellow group members, Brenda Praggastis, Melissa Stockman, Kaisa Taipale, Marilyn Vazquez, Sunny Wang, and Emily Winn. We'd especially like to thank Brenda Praggastis for her help preprocessing the time series data and setting up some of the code for the persistent homology analysis. We also thank Mathieu Chalifour for discussion of polysomnography time series. ST was partially funded by NSF grants DMS1800446 and CMMI-1800466. KS was partially funded by NSF grant DMS 1547357. GH would like to thank the National Sciences and Engineering Research Council of Canada (NSERC DG 2016-05167), Seed grant from Women and Children's Health Research Institute, Biomedical Research Award from American Association of Orthodontists Foundation, and the McIntyre Memorial fund from the School of Dentistry at the University of Alberta.

5 Appendix

This section contains figures referred to in the main article.

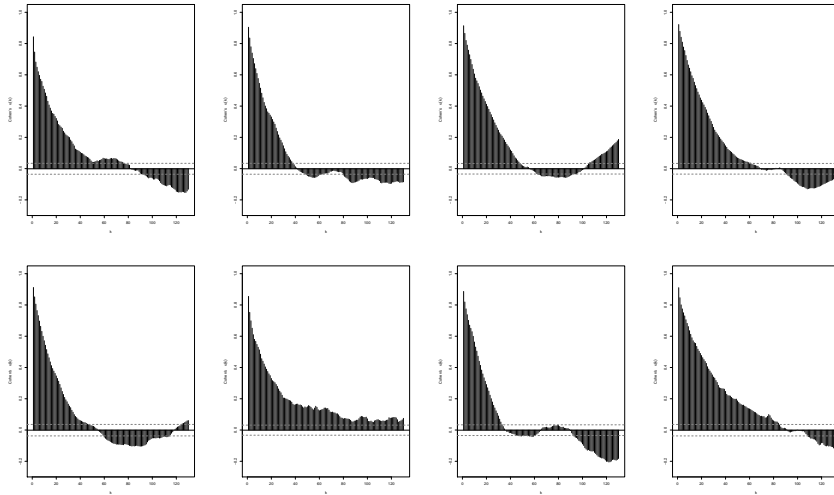


Fig. 12: Cohen's κ for patients, CF079 & CF076 (No OSA), CF030 & CF011 (Mild OSA), CF031 & CF046 (Moderate OSA), and CF055 & CF050 (Severe OSA) (from left to right and top to bottom.)

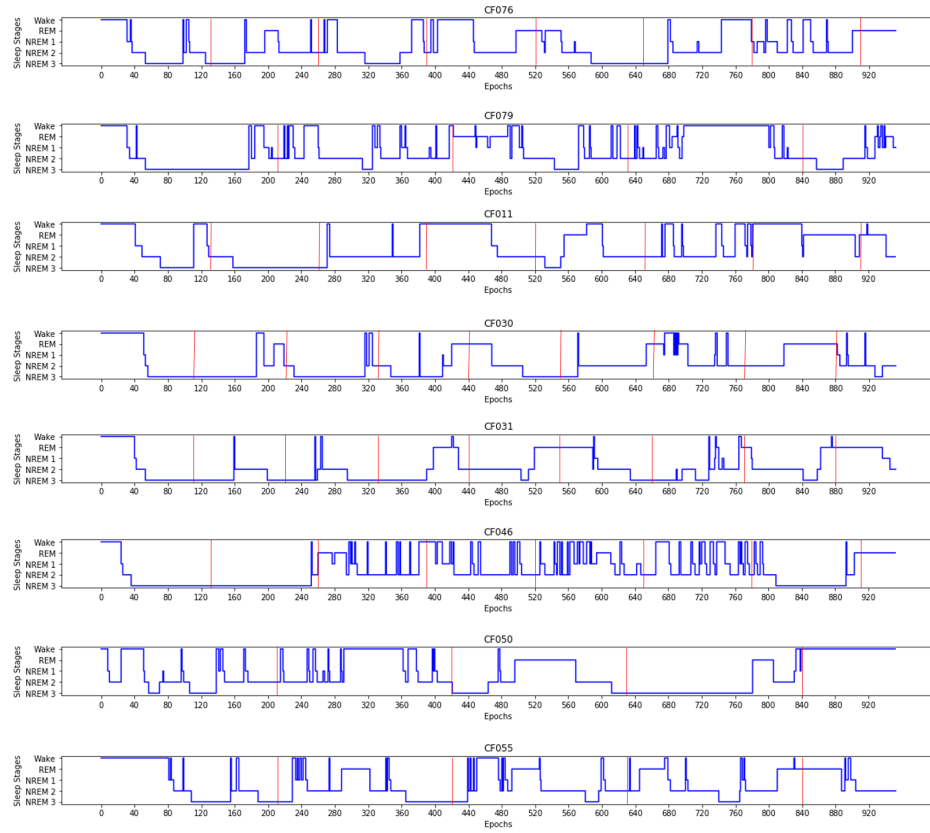


Fig. 13: Hypnograms of patients: CF079 & CF076 (No OSA), CF030 & CF011 (Mild OSA), CF031 & CF046 (Moderate OSA), and CF055 & CF050 (Severe OSA) with respective sleep cycles marked in red.

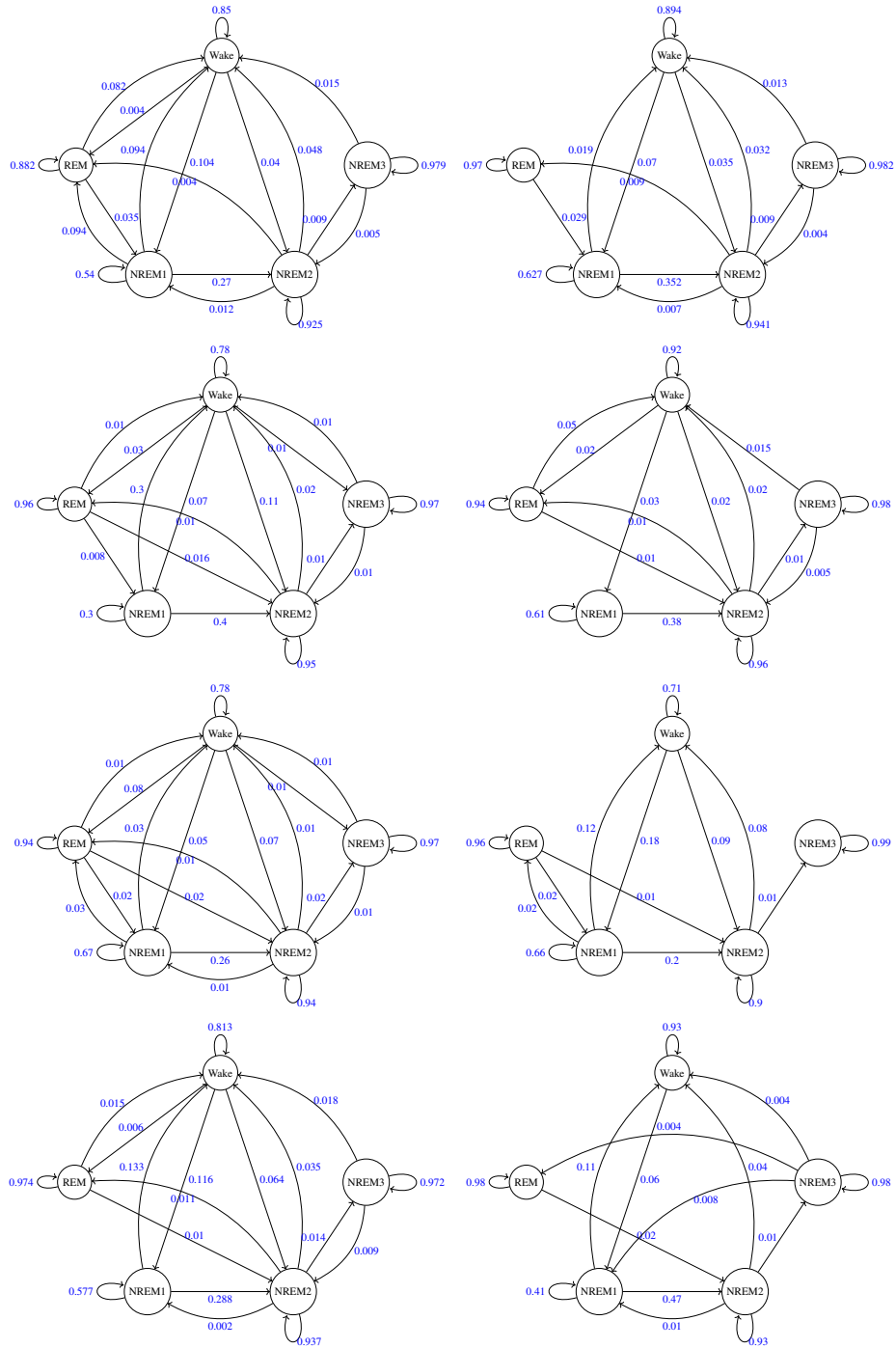


Fig. 14: Transition probabilities for patients CF079, CF076, CF030, CF031, CF046, CF055, and CF050 increasing order of *ahi* scores (left to right, and top to bottom).

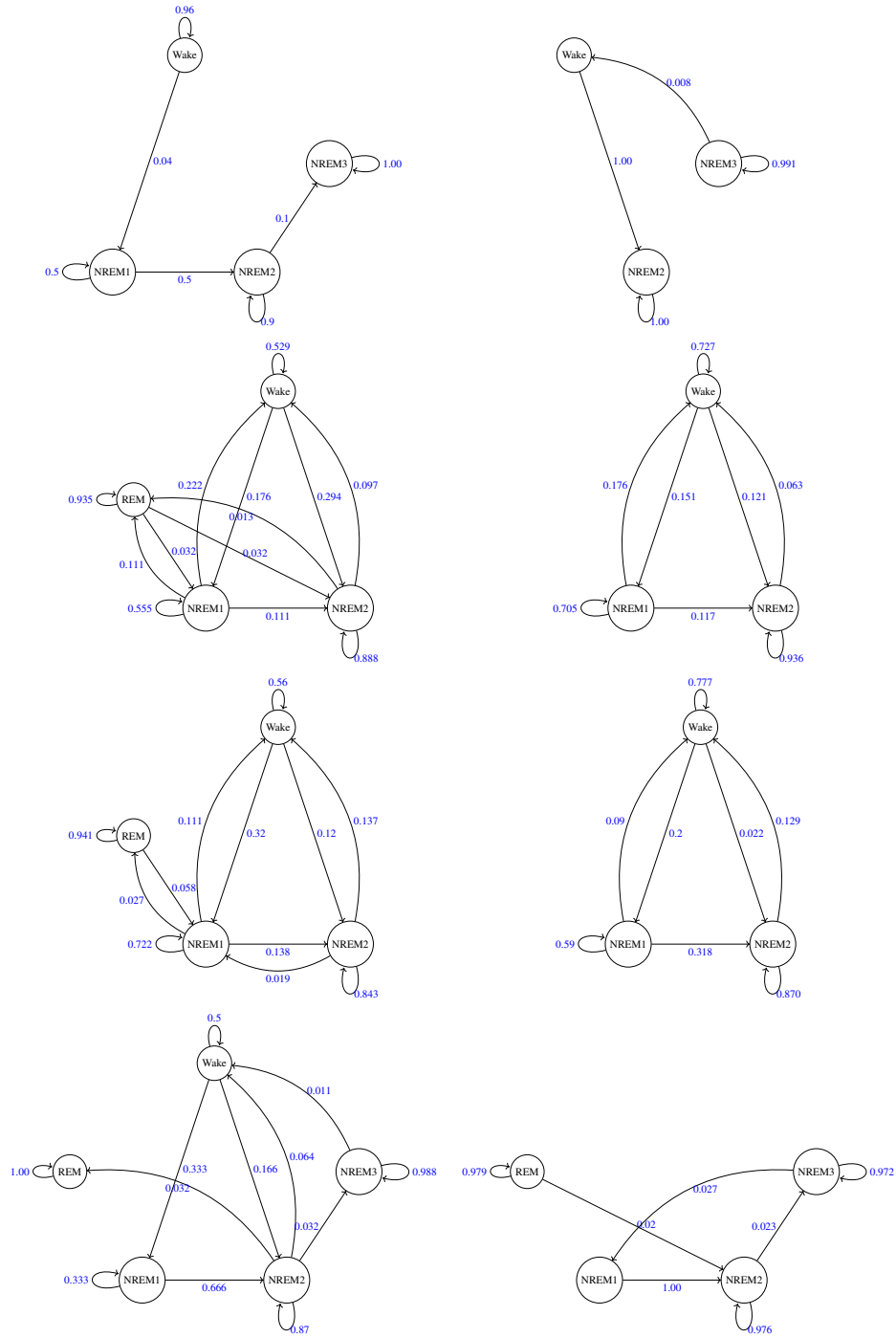


Fig. 15: Transition probabilities for the 8 sleep cycles of CF046 (displayed in order from left to right and top to bottom).

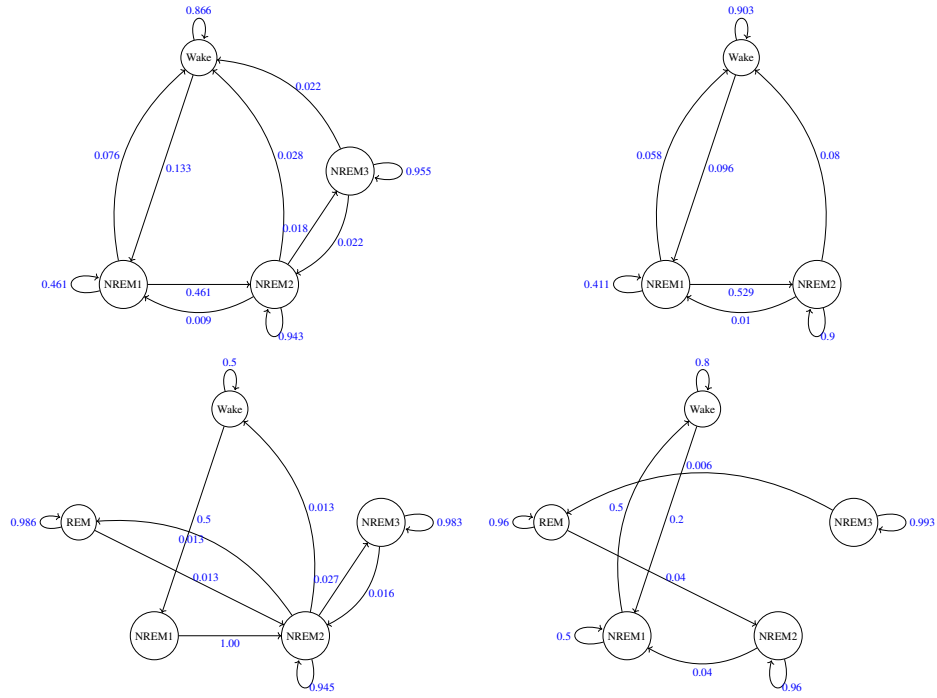


Fig. 16: Transition probabilities for the 4 sleep cycles of CF050 (displayed in order from left to right and top to bottom).

References

1. Henry Adams, Tegan Emerson, Michael Kirby, Rachel Neville, Chris Peterson, Patrick Shipman, Sofya Chepushtanova, Eric Hanson, Francis Motta, and Lori Ziegelmeier. Persistence images: A stable vector representation of persistent homology. *The Journal of Machine Learning Research*, 18(1):218–252, January 2017.
2. Jesse Berwald and Marian Gidea. Critical transitions in a model of a genetic regulatory system. *Mathematical Biosciences & Engineering*, 11(4):723–740, 2014.
3. Leo Breiman. Random forests. *Machine learning*, 45(1):5–32, 2001.
4. Leo Breiman. *Classification and regression trees*. Routledge, 2017.
5. Yu-Min Chung, Chuan-Shen Hu, Yu-Lun Lo, and Hau-Tieng Wu. A persistent homology approach to heart rate variability analysis with an application to sleep-wake classification. *arXiv preprint arXiv:1908.06856*, 2019.
6. Herbert Edelsbrunner and John Harer. *Computational Topology: An Introduction*. American Mathematical Society, 2010.
7. Jerome H Friedman. Greedy function approximation: a gradient boosting machine. *Annals of statistics*, pages 1189–1232, 2001.
8. Jacob Goldberger, Geoffrey E Hinton, Sam T Roweis, and Russ R Salakhutdinov. Neighbourhood components analysis. In *Advances in neural information processing systems*, pages 513–520, 2005.
9. Allen Hatcher. *Algebraic Topology*. Cambridge University Press, 2002.
10. Arthur E Hoerl and Robert W Kennard. Ridge regression: Biased estimation for nonorthogonal problems. *Technometrics*, 12(1):55–67, 1970.
11. Firas A. Khasawneh and Elizabeth Munch. Chatter detection in turning using persistent homology. *Mechanical Systems and Signal Processing*, 70-71:527–541, 2016.
12. Firas A. Khasawneh and Elizabeth Munch. Utilizing topological data analysis for studying signals of time-delay systems. In *Advances in Delays and Dynamics*, pages 93–106. Springer International Publishing, 2017.
13. Firas A. Khasawneh, Elizabeth Munch, and Jose A. Perea. Chatter classification in turning using machine learning and topological data analysis. In Tamas Insperger, editor, *14th IFAC Workshop on Time Delay Systems TDS 2018: Budapest, Hungary, 2830 June 2018*, volume 51, pages 195–200, 2018.
14. S. Kullback and R.A. Leibler. On Information and Sufficiency. *The Annals of Mathematical Statistics*, 3 1951.
15. Gidea M. Topological data analysis of critical transitions in financial networks. In Puzis R. Shmueli E., Barzel B., editor, *3rd International Winter School and Conference on Network Science NetSci-X 2017*, Springer Proceedings in Complexity. Springer, Cham, 2017.
16. Elizabeth Munch. A user’s guide to topological data analysis. *Journal of Learning Analytics*, 4(2), 2017.
17. Audun Myers and Firas Khasawneh. On the automatic parameter selection for permutation entropy. *arXiv preprint arXiv:1905.06443*, 2019.
18. Steve Y. Oudot. *Persistence Theory: From Quiver Representations to Data Analysis (Mathematical Surveys and Monographs)*. American Mathematical Society, 2015.
19. F. Pedregosa, G. Varoquaux, A. Gramfort, V. Michel, B. Thirion, O. Grisel, M. Blondel, P. Prettenhofer, R. Weiss, V. Dubourg, J. Vanderplas, A. Passos, D. Cournapeau, M. Brucher, M. Perrot, and E. Duchesnay. Scikit-learn: Machine learning in Python. *Journal of Machine Learning Research*, 12:2825–2830, 2011.
20. Musa Peker. A new approach for automatic sleep scoring: Combining taguchi based complex-valued neural network and complex wavelet transform. *Computer Methods and Programs in Biomedicine*, 129:203–216, jun 2016.
21. José A. Perea and John Harer. Sliding windows and persistence: An application of topological methods to signal analysis. *Foundations of Computational Mathematics*, pages 1–40, 2015.
22. Allan Rechtschaffen and Anthony Kales. A manual of standardized terminology, techniques and scoring system for sleep stages of human subjects: A. rechtschaffen and a. kales (editors). (public health service, u.s. government printing office, washington, d.c.). 1968.

23. Nathaniel Saul and Chris Tralie. Scikit-tda: Topological data analysis for python, 2019.
24. Johan AK Suykens and Joos Vandewalle. Least squares support vector machine classifiers. *Neural processing letters*, 9(3):293–300, 1999.
25. Floris Takens. Detecting strange attractors in turbulence. In *Lecture Notes in Mathematics*, pages 366–381. Springer Berlin Heidelberg, 1981.
26. Christopher Tralie. High-dimensional geometry of sliding window embeddings of periodic videos. In *32nd International Symposium on Computational Geometry (SoCG 2016)*. Schloss Dagstuhl-Leibniz-Zentrum fuer Informatik, 2016.
27. Christopher Tralie, Nathaniel Saul, and Rann Bar-On. Ripser.py: A lean persistent homology library for python. *The Journal of Open Source Software*, 3(29):925, Sep 2018.
28. Christopher J Tralie and Jose A Perea. (quasi) periodicity quantification in video data, using topology. *SIAM Journal on Imaging Sciences*, 11(2):1049–1077, 2018.
29. Christian H Weiss. *An Introduction to DiscreteValued Time Series*. John Wiley & Sons, Ltd, 2018.